ARTICLES

# Enhancement of proteasome activity by a small-molecule inhibitor of USP14

Byung-Hoon Lee[1]*, Min Jae Lee[1]*, Soyeon Park[1], Dong-Chan Oh[2,3], Suzanne Elsasser[1], Ping-Chung Chen[4], Carlos Gartner[1]†, Nevena Dimova[1], John Hanna[1]†, Steven P. Gygi[1], Scott M. Wilson[4], Randall W. King[1] & Daniel Finley[1]

**Proteasomes, the primary mediators of ubiquitin–protein conjugate degradation, are regulated through complex and poorly understood mechanisms. Here we show that USP14, a proteasome-associated deubiquitinating enzyme, can inhibit the degradation of ubiquitin–protein conjugates both *in vitro* and in cells. A catalytically inactive variant of USP14 has reduced inhibitory activity, indicating that inhibition is mediated by trimming of the ubiquitin chain on the substrate. A high-throughput screen identified a selective small-molecule inhibitor of the deubiquitinating activity of human USP14. Treatment of cultured cells with this compound enhanced degradation of several proteasome substrates that have been implicated in neurodegenerative disease. USP14 inhibition accelerated the degradation of oxidized proteins and enhanced resistance to oxidative stress. Enhancement of proteasome activity through inhibition of USP14 may offer a strategy to reduce the levels of aberrant proteins in cells under proteotoxic stress.**

The proteasome is essential for life in eukaryotes and regulates many aspects of cell physiology[1,2]. Substrates are targeted to the proteasome most often by means of ubiquitination. The proteasome holoenzyme is composed of a 19-subunit regulatory particle (known as the RP, 19S complex, or PA700) and a 28-subunit core particle (known as the CP or 20S complex). Substrate first binds the RP, and is then actively translocated to the CP, where it is degraded. The mechanisms regulating proteasome activity remain poorly understood, but involve numerous proteins that reversibly associate with it. Some bind the RP and deliver ubiquitin conjugates to the proteasome, whereas others open the axial channel into the CP. A third class of associated proteins, composed of ubiquitin ligases and deubiquitinating enzymes (DUBs), modifies proteasome-bound ubiquitin chains. Ubiquitin chains vary in their linkage type and length, and longer variants interact more strongly with the proteasome[3]. The extension and disassembly of chains at the proteasome may alter substrate degradation rates by changing substrate affinity for the proteasome.

Mammalian proteasomes are associated with three DUBs: RPN11, UCH37 and USP14 (refs 4–22). UCH37 and USP14 associate reversibly with the proteasome, whereas RPN11 is a stoichiometric subunit[1]. These enzymes reside on the RP and remove ubiquitin from the substrate before substrate degradation. The release of ubiquitin spares it from degradation, minimizing fluctuations in ubiquitin pools. The activity of RPN11 on the substrate's ubiquitin chain is thought to be delayed until the proteasome is committed to degrading the substrate[4,5]. RPN11 then cuts at the base of a ubiquitin chain, freeing substrate[5]. Thus, removal of the ubiquitin chain by RPN11 can promote substrate translocation into the CP to be hydrolysed[4,5]. However, deubiquitination before commitment might inhibit substrate degradation, as ubiquitin targets the protein for degradation[6].

In contrast to RPN11, USP14 and UCH37 can attack ubiquitin chains independently of commitment to substrate degradation. UCH37, and perhaps USP14, disassemble the chain from its substrate-distal tip[6,15,16], thus shortening chains rather than removing them en bloc. Little is known about such 'chain-trimming' reactions[6–8]. One model is that chain trimming increases the ability of proteasomes to discriminate between long and short multiubiquitin chains[6]. Here we show that a small-molecule inhibitor of deubiquitination by USP14 stimulates protein degradation *in vitro* and in cells. These findings reveal that, for those substrates tested, proteasome function is limited by USP14-dependent chain trimming. Thus, otherwise competent substrates of the proteasome can be rejected when chain trimming is faster than competing steps leading to substrate degradation.

## USP14 inhibits the proteasome *in vitro*

We have previously shown that Ubp6, the yeast orthologue of USP14, is a potent inhibitor of the proteasome[16]. To test whether this is also true of USP14 from humans, we first developed a purification procedure that results in proteasomes lacking detectable USP14 (modified from ref. 23). Such proteasomes retain high levels of ubiquitin-7-amido-4-methylcoumarin (Ub–AMC) hydrolysing activity (data not shown), which is presumably UCH37-dependent (Supplementary Fig. 1). This activity can be inhibited irreversibly using ubiquitin–vinylsulphone (Ub–VS)[24], which forms an adduct with the active site Cys in DUBs of the thiol protease class. When such 'VS-proteasomes' were reconstituted with recombinant USP14 (Supplementary Fig. 2), Ub–AMC hydrolysing activity was increased 800-fold over that of isolated USP14 (Fig. 1a). Thus, the deubiquitinating activity of USP14 is activated by proteasomes (see also refs 10, 11, 15, 18, 22). Using the Ub–AMC assay, the affinity of USP14 for the proteasome was found to be 4 nM (Supplementary Fig. 3).

Proteasomes reconstituted with a saturating amount of USP14 were challenged with a model proteasome substrate, ubiquitinated

[1]Department of Cell Biology, Harvard Medical School, 240 Longwood Avenue, Boston, Massachusetts 02115, USA. [2]Department of Biological Chemistry and Molecular Pharmacology, Harvard Medical School, 240 Longwood Avenue, Boston, Massachusetts 02115, USA. [3]Natural Products Research Institute, College of Pharmacy, Seoul National University, San 56-1, Sillim, Seoul 151-742, Republic of Korea. [4]Department of Neurobiology, Evelyn F. McKnight Brain Institute, Civitan International Research Center, University of Alabama at Birmingham, Birmingham, Alabama 35294, USA. †Present addresses: Department of Biological Sciences, 193 Galvin Life Sciences Center, Notre Dame, Indiana 46556, USA (C.G.); Department of Pathology, Brigham and Women's Hospital, 75 Francis Street, Boston, Massachusetts 02115, USA (J.H.).
*These authors contributed equally to this work.

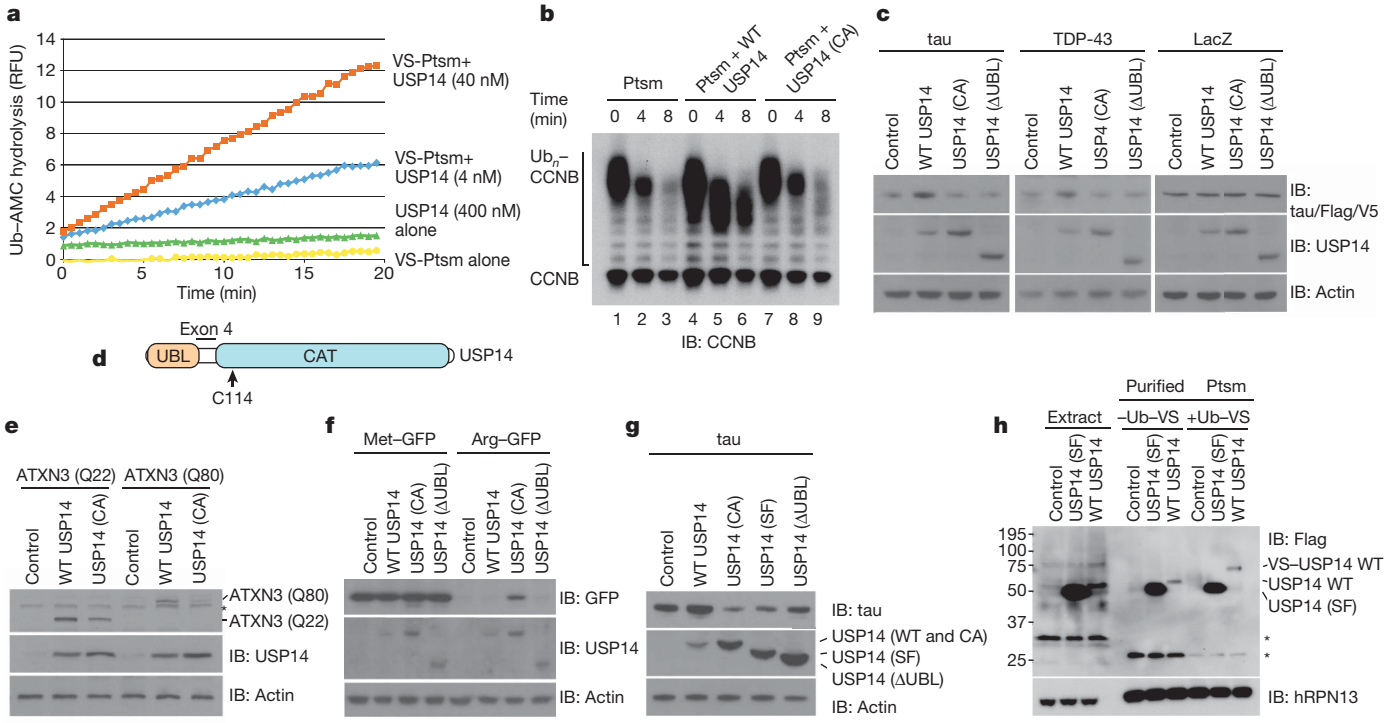


**Figure 1 | USP14 is an inhibitor of the proteasome.** **a**, Ub–AMC hydrolysis assay of USP14 activity in the presence or absence of Ub–VS-treated human proteasome (VS-proteasome; 1 nM). RFU, relative fluorescence units. Ptsm, 26S proteasome. **b**, *In vitro* degradation assay with polyubiquitinated CCNB (Ub$_n$–CCNB), human proteasome (4 nM), and wild-type (WT) USP14 (USP14) or mutant USP14(C114A) (USP14(CA); 60 nM). Samples in **b**, **c** and **e**–**h** were analysed by SDS–PAGE/immunoblotting (IB). **c**, Plasmids expressing tau, Flag–TDP-43, or V5–LacZ were co-transfected into *Usp14*$^{-/-}$ MEFs with variants of Flag–USP14 as indicated. Samples were collected 2 days after transfection. Actin, loading control. **d**, Diagram of human USP14, showing ubiquitin-like (UBL) and catalytic (CAT) domains. C114, active site cysteine. Splice variant USP14(SF) is produced from an mRNA lacking exon 4 (ref. 12). **e**, Flag-tagged ATXN3(Q22) or ATXN3(Q80) was co-expressed with USP14 variants in *Usp14*$^{-/-}$ MEFs and detected with anti-Flag antibodies. **f**, Arg–GFP or control Met–GFP co-expressed with USP14 variants in *Usp14*$^{-/-}$ MEFs. **g**, As **c** except HEK293 cells were used. **h**, USP14(SF) associates with but is not activated by proteasomes. Each variant of Flag–USP14 was expressed in HEK293T cells containing tagged hRPN11, and proteasomes were affinity purified. Where indicated, Ub–VS was incubated with lysate before proteasome purification. Extract samples represent 5% of total. Asterisks indicate nonspecific signals. Proteasome subunit hRPN13, loading control. Control samples, empty vector. Equal cell numbers were used for each lane.

cyclin B (Ub–CCNB). Like Ubp6, USP14 inhibited the degradation of Ub–CCNB (Fig. 1b). An active site mutant of USP14, USP14(C114A), showed little inhibitory effect, indicating that chain trimming is the basis for inhibition. Indeed, extensive trimming of ubiquitin from CCNB, as indicated by the shift of Ub–CCNB bands to a lower molecular mass, was evident in the presence of USP14 but not USP14(C114A) (Fig. 1b). Apparently, complete deubiquitination of CCNB is not required to suppress degradation, because USP14 rapidly removed only a portion of the ubiquitin from CCNB, even upon longer incubation (Fig. 1b). The strong dependence of chain trimming on USP14 was unexpected because active UCH37 was present in these proteasomes (Supplementary Fig. 1). When Ub–AMC is used as a substrate, UCH37 activity predominates over that of USP14 (refs 7, 8), but a true ubiquitin–protein conjugate, Ub–CCNB, shows the inverse effect. The lack of significant inhibition of degradation seen with USP14(C114A) was also surprising because Ubp6 exhibits a non-catalytic mechanism of proteasome inhibition[16]. As described below, a non-catalytic effect is seen with USP14, although it is not well visualized in this assay.

## USP14 inhibits protein turnover in cells

To verify that USP14 inhibits the proteasome in cells, we expressed USP14 variants in *Usp14*$^{-/-}$ murine embryonic fibroblasts (MEFs), together with proteasome substrates. As substrates we initially chose two proteins that are critical in neurodegenerative diseases: tau and TDP-43 (refs 25, 26). Tau is thought to undergo proteasomal degradation[27,28]. Tau and TDP-43 showed increased levels when co-expressed with wild-type USP14 in *Usp14*$^{-/-}$ MEFs, indicating proteasome inhibition by USP14 (Fig. 1c). No effect was seen at the mRNA level (Supplementary Fig. 4). As seen *in vitro*, USP14(C114A) showed little or no activity in the assay. Thus, the ability of the proteasome to degrade tau and TDP-43 in MEFs seems to be suppressed by trimming of ubiquitin from these substrates. The amino-terminal ubiquitin-like (UBL) domain of USP14 (Fig. 1d) is its principal proteasome-binding site[15], and accordingly deletion of the UBL domain abrogated the USP14 effect (Fig. 1c). The effects on tau levels reflected accelerated degradation: tau disappeared more slowly from cells expressing USP14 in a chase experiment (Supplementary Fig. 5). USP14 did not affect the levels of two proteins that are thought to be stable: LacZ and actin (Fig. 1c). In MEFs and other cell types, wild-type USP14 was usually expressed at lower levels than USP14(C114A) (Fig. 1), indicating that USP14 may be subject to autoregulation.

Another protein linked to neurodegeneration and thought to be a substrate of the proteasome is ataxin-3 (ATXN3)[29]. Polyglutamine-expanded forms of ATXN3 give rise to spinocerebellar ataxia 3. Both wild-type (22 glutamines; Q22) and expanded forms of ATXN3(Q80) were stabilized by expression of USP14 in *Usp14*$^{-/-}$ MEFs (Fig. 1e). Expression of wild-type USP14 engendered stronger accumulation of ATXN3 than expression of USP14(C114A). However, in contrast to tau and TDP-43, the stabilizing effect of catalytically inactive USP14 was substantial for ATXN3(Q22) and ATXN3(Q80). Stabilization of ATXN3 by USP14(C114A) presumably represents the same non-catalytic effect as described for Ubp6 in *Saccharomyces cerevisiae*[16]. Thus, the non-catalytic inhibitory effect is apparently conserved in evolution. A non-catalytic effect was also observed for a model substrate of the proteasome[30,31], Arg–GFP (Fig. 1f). Wild-type USP14 was

ineffective in Arg–GFP stabilization in comparison to USP14(C114A) (Fig. 1f), the non-catalytic effect being dominant. Met–GFP, a stable protein, was unaffected by USP14. It will be interesting to determine what substrate features underlie the differing sensitivities of these substrates to catalytic and non-catalytic inhibition of degradation.

The effect of USP14 on tau degradation was confirmed in HEK293 cells. As in MEFs, USP14 overexpression stabilized tau (Fig. 1g). Results obtained with USP14 mutants differed from those obtained using MEFs, as expected, given that HEK293 cells express endogenous USP14; the expression of USP14(C114A) in *Usp14*$^{-/-}$ MEFs had no effect on tau, whereas in HEK293 cells the USP14(C114A) mutant produced accelerated tau degradation (Fig. 1g). This result presumably reflects displacement of endogenous USP14 from the proteasome. As expected, deletion of the UBL domain attenuated the dominant-negative effect (Fig. 1g). In contrast to USP14(ΔUBL), the short form (SF) of USP14—expressed from a developmentally regulated[18] mRNA that lacks a 33-codon junctional exon (exon 4) between the UBL domain and the catalytic domain[12,18] (Fig. 1d)—did exhibit a dominant-negative effect (Fig. 1g). This result indicated that USP14(SF) might bind proteasomes and counter the action of full-length USP14. Thus, USP14(SF) may be an endogenous inhibitor of USP14 activity. Consistent with this possibility, USP14(SF) binds proteasomes, but is not activated enzymatically by proteasome binding, as shown by its inability to react with Ub–VS (Fig. 1h). USP14(SF) also seems to lack non-catalytic proteasome-inhibitory capacity, because its expression in *Usp14*$^{-/-}$ MEFs did not stabilize Arg–GFP (Supplementary Fig. 6).

## A selective small-molecule inhibitor of USP14

The results above suggested that chain trimming at the proteasome antagonizes the degradation of multiple substrates. Therefore, a small-molecule inhibitor of USP14 might enhance proteasome activity. We screened 63,052 compounds for the ability to inhibit USP14, using VS-proteasomes reconstituted with USP14 and assayed with Ub–AMC, identifying 215 as true USP14 inhibitors (details in Methods, Supplementary Table and Supplementary Fig. 7). When the hits were counter-screened against a panel of DUBs, only three of the strong hits showed selectivity for USP14. We proceeded with more detailed studies of the strongest hit, 1-[1-(4-fluorophenyl)-2,5-dimethylpyrrol-3-yl]-2-pyrrolidin-1-ylethanone, referred to hereafter as IU1 (Fig. 2a). Its structure is suggestive of an active-site-directed thiol protease inhibitor. The half-maximal inhibitory concentration ($IC_{50}$) of IU1 for USP14 is 4–5 μM (Fig. 2b and Supplementary Fig. 8). IU1 failed to significantly inhibit eight DUBs of human origin (Fig. 2b, c and Supplementary Figs 9 and 10), as well as Ub–AMC hydrolysis by proteasomes lacking USP14, which is attributable to UCH37 (Supplementary Fig. 8). We also identified a compound that is closely related to IU1 but does not inhibit USP14 (IU1C; Fig. 2a and Supplementary Fig. 11), and used this as a specificity control in subsequent assays. In the absence of proteasomes, USP14 was insensitive to IU1 (Supplementary Fig. 8), indicating that IU1 binds specifically to the activated form of USP14. IU1 could potentially inhibit USP14 by preventing its docking on the proteasome, but direct tests of this scenario proved negative (Supplementary Fig. 12). USP14 inhibition was rapidly established upon addition of IU1 and rapidly reversed upon its removal (Fig. 2d and Supplementary Fig. 13).

We used Ub–CCNB to test whether IU1 could inhibit the trimming of ubiquitin chains by the proteasome. To separate chain trimming from substrate degradation, these assays were done in the presence of proteasome inhibitors[4]. When proteasomes lacking USP14 were tested, IU1 had no effect on ubiquitin chain trimming (Fig. 3a). Chain trimming was strongly enhanced by USP14, as apparent from the increased electrophoretic mobility of Ub–CCNB species. Addition of IU1 to the assay reversed this effect (Fig. 3a; see also Supplementary Fig. 14).

We next tested whether IU1 could enhance degradation. Proteasomal degradation of Ub–CCNB was indeed markedly stimulated by IU1 (Fig. 3b). Proteasomes lacking USP14 were insensitive to IU1 (Fig. 3b), and CCNB degradation was unaffected by IU1 when proteasomes were reconstituted with USP14(C114A) (Supplementary Fig. 15). Thus, suppression of chain trimming by IU1 may account for its enhancement of degradation. IU1 also promoted degradation of Sic1, a CDK inhibitor from *S. cerevisiae* (Fig. 3c). These assays used a modified form of Sic1 in which the PY element signals ubiquitination[32]. Both substrates used in these *in vitro* assays, Ub–CCNB and Sic1, carry mixed ubiquitin chains, including linkages via K48, K63 and K11 residues[32,33]. Whether chains of different topologies vary in their susceptibility to USP14-dependent regulation is an important issue for future study.

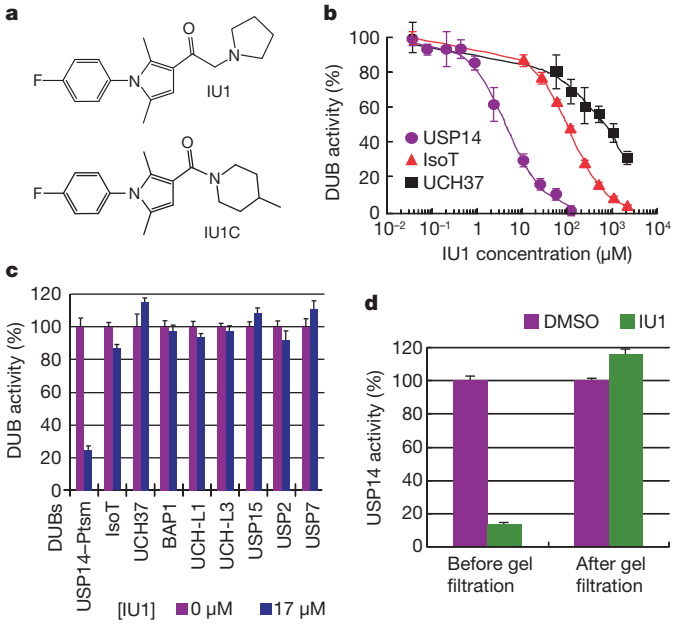


**Figure 2 | IU1 inhibits human USP14 specifically and reversibly.** **a**, Chemical structures of IU1 and IU1C. Analytical data shown in Supplementary Fig. 16. **b**, $IC_{50}$ determination for IU1 inhibition of Ub–AMC hydrolysis by proteasome-bound USP14 (4.7 ± 0.7 μM), IsoT (100 ± 0.4 μM) and UCH37 (700 ± 300 μM). **c**, Ub–AMC (1 μM) hydrolysis assays showing specificity of IU1 for USP14 in comparison to eight other DUB enzymes. **d**, Reversibility of USP14 inhibition. 60 nM USP14 and 5 nM human proteasome were treated with vehicle (DMSO) or 100 μM IU1 for 2 h. After rapid spin gel-filtration, proteins were assayed for Ub–AMC hydrolysis. All values are presented as mean ± s.d. ($n = 3$).

## A USP14 inhibitor accelerates proteolysis in cells

To determine whether IU1 is cell permeable, it was added to cultures and cell-associated IU1 was quantified by liquid chromatography-mass spectrometry (LC-MS) or ultraviolet absorption. When added at 50 μM, IU1 reached an apparent intracellular concentration of ~13 μM within 1 h, which remained constant over the course of the experiment (Supplementary Figs 17–19). Effects of IU1 on the viability of MEFs only became apparent at 250 μM (Supplementary Figs 20 and 21). Moreover, IU1 did not noticeably induce apoptosis (Supplementary Fig. 22). When cell proliferation was measured in real time, slight inhibition became apparent at 120 μM (Supplementary Fig. 21). In the case of both cell viability and proliferation assays, *Usp14*$^{-/-}$ MEFs were no less sensitive than wild type, indicating that IU1 toxicity at high concentrations was independent of USP14 inhibition.

To determine whether IU1 could enhance proteasome function in cells, we expressed tau in MEFs treated with sub-cytotoxic doses of IU1. IU1 induced dose-dependent reduction in tau levels, with a strong effect seen at 50 μM (Fig. 4a and Supplementary Fig. 23). Thus, IU1 treatment affected tau similarly to USP14(C114A) (Fig. 1c), consistent with active site inhibition. No effect was seen on tau mRNA (Supplementary Fig. 24). When *Usp14*$^{-/-}$ MEFs were

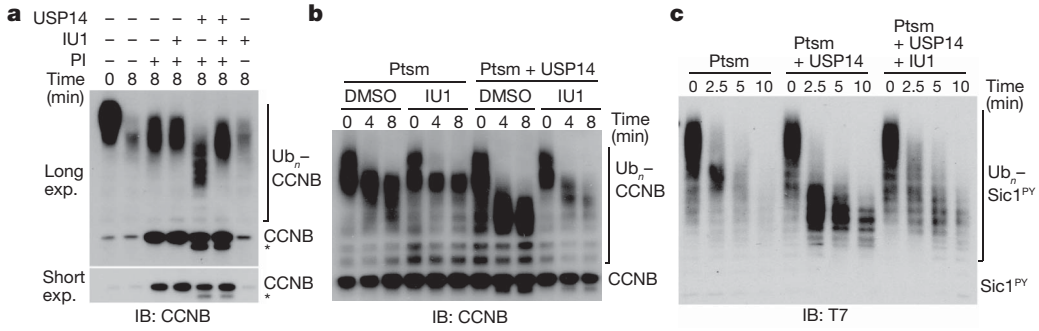


**Figure 3 | IU1 inhibits chain trimming and stimulates substrate degradation *in vitro*.** **a**, Chain-trimming assays. Samples contained 4 nM proteasome, and USP14 was added at 15-fold molar excess over proteasome. IU1 was added at 50 μM and proteasome inhibitors (PI) at 5 μM (PS-341, epoxomicin). Asterisk indicates CCNB species derived from residual thrombin from USP14 preparation[16]. All panels, SDS–PAGE/immunoblot analysis. **b**, *In vitro* $Ub_n$–CCNB degradation assay (IU1 at 34 μM). **c**, *In vitro* degradation assay with polyubiquitinated, T7-tagged $Sic1^{PY}$, human proteasome (5 nM) and wild-type USP14 (75 nM) in the absence or presence of IU1 (75 μM).

treated with IU1, no effect on tau was observed, indicating that IU1 enhances tau degradation through inhibiting USP14 (Fig. 4b). On the basis of these and previous experiments (Fig. 2c), nonspecific inhibition of other DUBs by IU1 does not affect proteasome function at this dose. The effect of IU1 on tau degradation was independent of autophagy (Supplementary Fig. 25). Several other proteins implicated in proteotoxic mechanisms—TDP-43, ATXN3, and glial fibrillary acidic protein (GFAP)—were similarly depleted from MEFs by IU1 (Fig. 4d, e and Supplementary Fig. 26). The effectiveness of IU1 in neurons, where proteotoxic mechanisms are commonly observed, has not been examined.

IU1 enhanced the extent of ubiquitin modification of TDP-43 in cells, perhaps accounting for its accelerated degradation (Fig. 4f). In contrast, little change was seen in bulk cellular ubiquitin conjugates (Fig. 4g and Supplementary Fig. 27). Free ubiquitin was reduced after IU1 addition, and, as the dose of IU1 increased, the level of free ubiquitin in wild-type MEFs approached that of untreated $Usp14^{-/-}$ MEFs (Fig. 4g). Previous work showed that USP14 and Ubp6 assist in the maintenance of cellular ubiquitin pools by suppressing proteasomal degradation of ubiquitin[11,13,14,17,34,35]. The conjugated rather than free form of ubiquitin is most subject to degradation[36]. By separating ubiquitin from its conjugative target, USP14 antagonizes this pathway of ubiquitin degradation.

Enhanced protein degradation in cells treated with IU1 could result from increased synthesis of proteasomes; however, no significant changes in proteasome composition were seen after IU1 treatment (Supplementary Fig. 28). USP14 is known to regulate gating of the proteasome[21], but this does not seem to be critical in the mode of action of IU1 (B.-H.L. and D.F., unpublished data). The detailed similarities observed between the effects of mutational inactivation

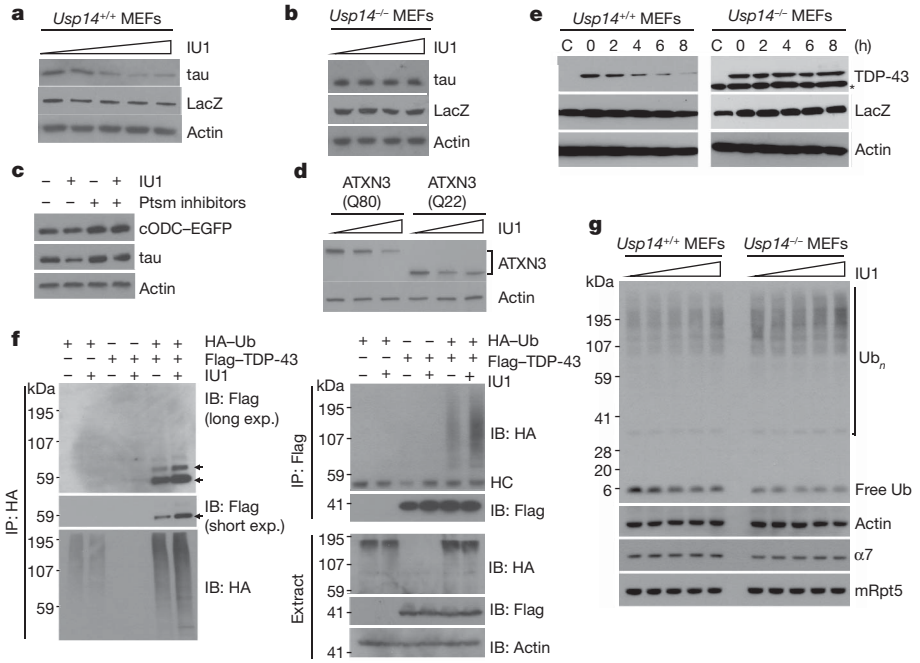


**Figure 4 | IU1 enhances proteasomal degradation in cells.** All panels show SDS–PAGE/immunoblot data. **a**, Thirty-six hours after co-transfecting wild-type MEFs with plasmids expressing tau and V5–LacZ, cells were incubated with 0, 25, 50, 75, or 100 μM of IU1 for 6 h. LacZ, transfection control. Actin, loading control. **b**, As in **a** except that MEFs were $Usp14^{-/-}$ and IU1 was at 0, 10, 50, or 100 μM. **c**, Tau and Ub-independent proteasome substrate cODC–EGFP were co-expressed in wild-type MEFs and incubated with 50 μM IU1 for 6 h. Proteasome inhibitors were MG132 (30 μM) and PS-341 (10 μM). **d**, As **b** except with ATXN3(Q80) and ATXN3(Q22), and IU1 at 0, 50 and 100 μM. **e**, Flag–TDP-43 was co-transfected with a LacZ-expressing plasmid into either wild-type or $Usp14^{-/-}$ MEFs, then treated with IU1 (75 μM) for the indicated time. Asterisk, nonspecific signal. **f**, HA-tagged Ub and/or Flag-tagged TDP-43 were transiently overexpressed in wild-type MEFs with 50 μM IU1 incubation for 6 h. Proteasome inhibitors (20 μM MG132, 10 μM PS-341) were added 4 h before lysis. Lysates were subjected to immunoprecipitation with anti-HA or anti-Flag. Arrows indicate likely ubiquitinated TDP-43 species. HC, heavy chain. **g**, Wild-type MEFs and $Usp14^{-/-}$ MEFs were treated with IU1 (0, 25, 50, 75, or 100 μM) for 6 h, followed by analysis for ubiquitin, actin, CP subunit α7 and RP subunit mRpt5.

of USP14's catalytic site and IU1 treatment, as well as the observation that USP14 is required for IU1 to affect protein degradation, provide strong evidence for the importance of chain trimming by USP14. In addition, IU1 had little or no effect in a cell-based assay on the degradation of a ubiquitin-independent substrate[37] of the proteasome, C-terminal ornithine decarboxylase-EGFP (cODC–EGFP) (Fig. 4c). Similar results were obtained *in vitro* with antizyme-promoted ODC degradation (data not shown). The effects of IU1 are probably restricted to ubiquitin-dependent proteasome substrates, based on its mode of action, but further characterization is required to establish this. Finally, Arg–GFP levels did not change upon treatment with IU1, when assayed in cells expressing USP14(C114A), indicating that IU1 does not influence USP14's non-catalytic inhibitory effect (Supplementary Fig. 26).

Oxidized proteins form a class of misfolded proteasome substrates that increase with age and are apparently toxic when they accumulate[38,39]. We induced protein oxidation by treating cells with menadione, and visualized oxidized species via their carbonyl groups. IU1 treatment strongly reduced the accumulation of oxidized proteins (Fig. 5a). When proteasome inhibitor was added, the effect of IU1 was attenuated, indicating that IU1 does not prevent the oxidation reaction itself. IU1 treatment reduced menadione toxicity substantially in HEK293 cells (Fig. 5b), strongly supporting the hypothesis that proteins are critical targets of oxidative damage. IU1 also reduced the toxicity of an unrelated oxidizing agent, hydrogen peroxide (data not shown). IU1C, the IU1 variant that is inactive against USP14, failed to reduce menadione cytotoxicity (Supplementary Fig. 29). These experiments suggest that IU1 can promote cell survival during proteotoxic stress.

### Ubiquitin chain trimming antagonizes proteasome function

We report here that a small molecule selected for its capacity to inhibit the proteasome-associated deubiquitinating enzyme USP14 strongly enhances substrate degradation by the proteasome in cells. This is the first evidence that chain trimming by USP14 or its yeast orthologue Ubp6 inhibits proteasome activity through deubiquitination. The trimming of substrate-bound ubiquitin chains on the proteasome seems to govern the degradation rates of many ubiquitin–protein conjugates. Under normal growth conditions, the proteasome may be subject to tonic inhibition through this mechanism.

The scope of proteasome inhibition by chain trimming is not limited to substrates bearing only one or a few ubiquitin groups[6], as shown by studies of cyclin B and $Sic1^{PY}$ degradation. Also, suppression of degradation by chain trimming does not seem to be restricted to proteins that are not proper substrates of the proteasome. Chain trimming may be a more general, although not universal, mechanism for regulating protein turnover rates, suppressing the degradation of some substrates but not others. Further work will be required to determine what fraction of proteasome substrates can be regulated through this pathway, and what distinguishing features they share.

We also report that USP14 can inhibit proteasome function non-catalytically, as previously observed for its yeast orthologue Ubp6 (ref. 16). The capacity of USP14 to inhibit proteasomes via two distinct pathways has important implications. Briefly, the non-catalytic effect, in slowing substrate degradation at the proteasome, may allow individual substrates to be docked at the proteasome for a longer time, thus resulting in more extensive trimming of ubiquitin chains. However, the two modes of proteasome inhibition are not obligatorily coupled, because proteasome substrates exhibited differing relative sensitivities to catalytic and non-catalytic inhibition by USP14 (Fig. 1c–f). It will be important to identify the mechanistic basis of these differences.

Both USP14 and UCH37 exhibit chain-trimming activity, but the effectiveness of IU1 in reducing chain trimming and stimulating proteasome activity suggests that the redundancy between these two proteasome-bound enzymes may be less than expected. UCH37 does not readily substitute for USP14. Proteasomes are associated with multiple ubiquitin receptors, and the relative susceptibility of substrates to chain trimming by USP14 and UCH37 may depend on which receptors are engaged with a given substrate and the positioning of these receptors with respect to USP14 and UCH37. For example, UCH37 binds proteasomes via a ubiquitin receptor, RPN13 (refs 24, 40–42). Whether chain trimming by UCH37 can suppress proteasome activity as powerfully as USP14 will require further study.

Although eukaryotic cells require proteasome function, proteasome inhibitors have proven highly effective in the treatment of multiple myeloma[43], and may have additional applications[44]. In other contexts, however, enhancement of proteasome activity might be beneficial[45,46]. For example, enhanced proteasome function could have applications in disorders that result from partial loss-of-function mutations in ubiquitin pathway components[47]. More generally, many diseases, including major neurodegenerative diseases, are thought to be caused by the accumulation of misfolded proteins[48–50]. Misfolding, which renders these proteins toxic, can also mark them as substrates of the ubiquitin-proteasome and autophagy pathways[50]. Enhanced proteasome function, as induced by inhibitors of chain trimming, could therefore potentially be used to eliminate such toxic proteins more effectively.

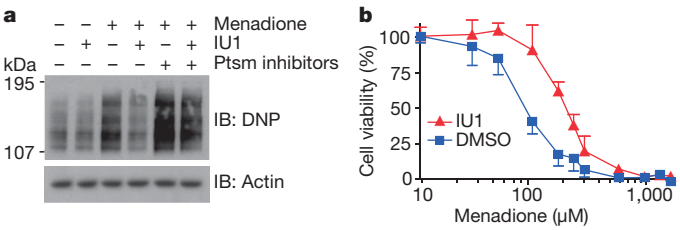


**Figure 5 | IU1 alleviates cytotoxicity induced by oxidative stress.** **a**, HEK293 cells were pre-incubated with IU1 (75 μM) or proteasome inhibitors (20 μM MG132, 10 μM PS-341) for 4 h, then treated with menadione (300 μM) for 60 min. Lysates were treated with DNPH and immunoblotted with anti-DNP antibody to assay oxidized proteins. **b**, Cell survival under oxidative stress measured using the MTT assay. HEK293 cells were pre-treated with 50 μM IU1 for 2 h. Menadione was added, followed by 4 h incubation. IU1 effects comparable to those of panels **a** and **b** were obtained in wild-type but not $Usp14^{-/-}$ MEFs (data not shown). Values are represented as mean ± s.d. ($n = 3$).

## METHODS SUMMARY

For expression in mammalian cells we used full-length USP14 (wild-type USP14) and its splice variant lacking exon 4 (USP14(SF)) subcloned into pcDNA3.1 (Invitrogen) as previously described[18]. The USP14(C114A) and USP14(ΔUBL) constructs were generated in the same vector by PCR-mediated mutagenesis and confirmed by sequencing. Human proteasomes were affinity-purified on a large scale from a stable HEK293 cell line harbouring HTBH-tagged hRPN11 (a gift from L. Huang). Ten microlitres of USP14 sample were dispensed into 384-well low volume plates in duplicate using a Wellmate dispenser. 33.3 nl of compound from the library were transferred into the wells using a Seiko pin transfer robotic system, followed by pre-incubation for ~30 min. To initiate the reaction, 10 μl of VS-proteasome plus Ub–AMC mixture were added to each well. The sources of compound libraries for screening were as follows: Maybridge, Asinex, ActiMol TimTec, ChemBridge, ChemDiv, Enamine and MMV1. Primary hits were defined by 'robust' *Z*-score analysis (Supplementary Fig. 7). To obtain dose–response curves, curve fitting was performed by the four parameter logistic model or the three parameter fixed bottom model using SigmaPlot 9.0 according to guidelines from NIH Chemical Genomics Center. The gene trap allele, $Usp14^{rrk114}$ (ref. 19), is referred to here as $Usp14^{-/-}$.

**Full Methods** and any associated references are available in the online version of the paper at www.nature.com/nature.

**Received 22 April; accepted 14 June 2010.**

1. Finley, D. Recognition and processing of ubiquitin-protein conjugates by the proteasome. *Annu. Rev. Biochem.* **78**, 477–513 (2009).
2. Schrader, E. K., Harstad, K. G. & Matouschek, A. Targeting proteins for degradation. *Nature Chem. Biol.* **5**, 815–822 (2009).

3. Thrower, J. S., Hoffman, L., Rechsteiner, M. & Pickart, C. M. Recognition of the polyubiquitin proteolytic signal. *EMBO J.* **19,** 94–102 (2000).
4. Verma, R. *et al.* Role of Rpn11 metalloprotease in deubiquitination and degradation by the 26S proteasome. *Science* **298,** 611–615 (2002).
5. Yao, T. & Cohen, R. E. A cryptic protease couples deubiquitination and degradation by the proteasome. *Nature* **419,** 403–407 (2002).
6. Lam, Y. A., Xu, W., DeMartino, G. N. & Cohen, R. E. Editing of ubiquitin conjugates by an isopeptidase in the 26S proteasome. *Nature* **385,** 737–740 (1997).
7. Koulich, E., Li, X. & DeMartino, G. N. Relative structural and functional roles of multiple deubiquitylating proteins associated with mammalian 26S proteasome. *Mol. Biol. Cell* **19,** 1072–1082 (2008).
8. Jacobson, A. D. *et al.* The lysine 48 and lysine 63 ubiquitin conjugates are processed differently by the 26S proteasome. *J. Biol. Chem.* **284,** 35485–35494 (2009).
9. Verma, R. *et al.* Proteasomal proteomics: identification of nucleotide-sensitive proteasome-interacting proteins by mass spectrometric analysis of affinity-purified proteasomes. *Mol. Biol. Cell* **11,** 3425–3439 (2000).
10. Borodovsky, A. *et al.* A novel active site-directed probe specific for deubiquitylating enzymes reveals proteasome association of USP14. *EMBO J.* **20,** 5187–5196 (2001).
11. Leggett, D. S. *et al.* Multiple associated proteins regulate proteasome structure and function. *Mol. Cell* **10,** 495–507 (2002).
12. Wilson, S. M. *et al.* Synaptic defects in ataxia mice result from a mutation in Usp14, encoding a ubiquitin-specific protease. *Nature Genet.* **32,** 420–425 (2002).
13. Chernova, T. A. *et al.* Pleiotropic effects of Ubp6 loss on drug sensitivities and yeast prion are due to depletion of the free ubiquitin pool. *J. Biol. Chem.* **278,** 52102–52115 (2003).
14. Anderson, C. *et al.* Loss of Usp14 results in reduced levels of ubiquitin in ataxia mice. *J. Neurochem.* **95,** 724–731 (2005).
15. Hu, M. *et al.* Structure and mechanisms of the proteasome-associated deubiquitinating enzyme Usp14. *EMBO J.* **24,** 3747–3756 (2005).
16. Hanna, J. *et al.* Deubiquitinating enzyme Ubp6 functions noncatalytically to delay proteasomal degradation. *Cell* **127,** 99–111 (2006).
17. Hanna, J., Meides, A., Zhang, D. P. & Finley, D. A ubiquitin stress response induces altered proteasome composition. *Cell* **129,** 747–759 (2007).
18. Crimmins, S. *et al.* Transgenic rescue of ataxia mice with neuronal-specific expression of ubiquitin-specific protease 14. *J. Neurosci.* **26,** 11423–11431 (2006).
19. Crimmins, S. *et al.* Transgenic rescue of ataxia mice reveals a male-specific sterility defect. *Dev. Biol.* **325,** 33–42 (2009).
20. Chen, P.-C. *et al.* The proteasome-associated deubiquitinating enzyme Usp14 is essential for the maintenance of synaptic ubiquitin levels and the development of neuromuscular junctions. *J. Neurosci.* **29,** 10909–10919 (2009).
21. Peth, A., Besche, H. C. & Goldberg, A. L. Ubiquitinated proteins activate the proteasome by binding to Usp14/Upb6, which cause 20S gate opening. *Mol. Cell* **36,** 794–804 (2009).
22. Catic, A. *et al.* Screen for ISG15-crossreactive deubiquitinases. *PLoS ONE* **2,** e679 (2007).
23. Wang, X. *et al.* Mass spectrometric characterization of the affinity-purified human 26S proteasome complex. *Biochemistry* **46,** 3553–3565 (2007).
24. Yao, T. *et al.* Proteasome recruitment and activation of the Uch37 deubiquitinating enzyme by Adrm1. *Nature Cell Biol.* **8,** 994–1002 (2006).
25. Spires-Jones, T. L., Stoothoff, W. H., de Calignon, A., Jones, P. B. & Hyman, B. T. Tau pathophysiology in neurodegeneration: a tangled issue. *Trends Neurosci.* **32,** 150–159 (2009).
26. Kwong, L. K., Uryu, K., Trojanowski, J. Q. & Lee, V. M. TDP-43 proteinopathies: neurodegenerative protein misfolding diseases without amyloidosis. *Neurosignals* **16,** 41–51 (2008).
27. David, D. C. *et al.* Proteasomal degradation of tau protein. *J. Neurochem.* **83,** 176–185 (2002).
28. Petrucelli, L. *et al.* CHIP and Hsp70 regulate tau ubiquitination, degradation and aggregation. *Hum. Mol. Genet.* **13,** 703–714 (2004).
29. Todi, S. V. *et al.* Cellular turnover of the polyglutamine disease protein ataxin-3 is regulated by its catalytic activity. *J. Biol. Chem.* **282,** 29348–29358 (2007).
30. Varshavsky, A., Turner, G., Du, F. & Xie, Y. The ubiquitin system and the N-end rule pathway. *Biol. Chem.* **381,** 779–789 (2000).
31. Dantuma, N. P., Lindsten, K., Glas, R., Jellne, M. & Masucci, M. G. Short-lived green fluorescent proteins for quantifying ubiquitin/proteasome-dependent proteolysis in living cells. *Nature Biotechnol.* **18,** 538–543 (2000).
32. Saeki, Y., Isono, E. & Toh-E, A. Preparation of ubiquitinated substrates by the PY motif-insertion method for monitoring proteasome activity. *Methods Enzymol.* **399,** 215–227 (2005).
33. Kirkpatrick, D. S. *et al.* Quantitative analysis of *in vitro* ubiquitinated cyclin B1 reveals complex chain topology. *Nature Cell Biol.* **8,** 700–710 (2006).
34. Amerik, A. Y., Li, S. J. & Hochstrasser, M. Analysis of the deubiquitinating enzymes of the yeast *Saccharomyces cerevisiae*. *Biol. Chem.* **381,** 981–992 (2000).
35. Hanna, J., Leggett, D. S. & Finley, D. Ubiquitin depletion as a key mediator of toxicity by translational inhibitors. *Mol. Cell. Biol.* **23,** 9251–9261 (2003).
36. Shabek, N., Herman-Bachinsky, Y. & Ciechanover, A. Ubiquitin degradation with its substrate, or as a monomer in a ubiquitination-independent mode, provides clues to proteasome regulation. *Proc. Natl Acad. Sci. USA* **106,** 11907–11912 (2009).
37. Hoyt, M. A., Zhang, M. & Coffino, P. Probing the ubiquitin/proteasome system with ornithine decarboxylase, a ubiquitin-independent substrate. *Methods Enzymol.* **398,** 399–413 (2005).
38. Stadtman, E. R. Protein oxidation and aging. *Free Radic. Res.* **40,** 1250–1258 (2006).
39. Ahmed, E. K., Picot, C. R., Bulteau, A. L. & Friguet, B. Protein oxidative modifications and replicative senescence of WI-38 human embryonic fibroblasts. *Ann. NY Acad. Sci.* **1119,** 88–96 (2007).
40. Hamazaki, J. *et al.* A novel proteasome interacting protein recruits the deubiquitinating enzyme UCH37 to 26S proteasomes. *EMBO J.* **25,** 4524–4536 (2006).
41. Qiu, X. B. *et al.* hRpn13/ADRM1/GP110 is a novel proteasome subunit that binds the deubiquitinating enzyme, UCH37. *EMBO J.* **25,** 5742–5753 (2006).
42. Husnjak, K. *et al.* Proteasome subunit Rpn13 is a novel ubiquitin receptor. *Nature* **453,** 481–488 (2008).
43. Chauhan, D., Bianchi, G. & Anderson, K. C. Targeting the UPS as therapy in multiple myeloma. *BMC Biochem.* **9** (Suppl. 1), S1 (2008).
44. Muchamuel, T. *et al.* A selective inhibitor of the immunoproteasome subunit LMP7 blocks cytokine production and attenuates progression of experimental arthritis. *Nature Med.* **15,** 781–787 (2009).
45. Chondrogianni, N. *et al.* Overexpression of proteasome β5 subunit increases the amount of assembled proteasome and confers ameliorated response to oxidative stress and higher survival rates. *J. Biol. Chem.* **280,** 11840–11850 (2005).
46. Tonoki, A. *et al.* Genetic evidence linking age-dependent attenuation of the 26S proteasome with the aging process. *Mol. Cell. Biol.* **29,** 1095–1106 (2009).
47. Lehman, N. L. The ubiquitin proteasome system in neuropathology. *Acta Neuropathol.* **118,** 329–347 (2009).
48. Hinault, M. P., Ben-Zvi, A. & Goloubinoff, P. Chaperones and proteases: cellular fold-controlling factors of proteins in neurodegenerative diseases and aging. *J. Mol. Neurosci.* **30,** 249–265 (2006).
49. Balch, W. E., Morimoto, R. I., Dillin, A. & Kelly, J. W. Adapting proteostasis for disease intervention. *Science* **319,** 916–919 (2008).
50. Goldberg, A. L. Protein degradation and protection against misfolded and damaged proteins. *Nature* **426,** 895–899 (2003).


**Supplementary Information** is linked to the online version of the paper at www.nature.com/nature.

**Acknowledgements** We thank K. Gordon, J. Y. Suk and N. Bays for advice and assistance, and members of the Finley laboratory for comments on the manuscript. We thank C. Shamu and the staff of the ICCB facility at Harvard Medical School, where the HT screen was carried out. We also thank N. Hathaway for ubiquitinated cyclin B, L. Huang for the tagged proteasome cell line, R. Baker for anti-USP14 antibody, G. DeMartino for anti-UCH37 antibody, K. Wilkinson and K. Walters for DUB enzymes, as well as C. Seong, M. Kim, S. M. Lim and D. Waterman for assistance in some experiments. For plasmids, we thank K. Walters, M. Sowa, W. Harper, V. Lee, F. Baralle, H. Paulson, Y. T. Kwon, M. Masucci, M.-K. Kwak, P. Coffino and C. Kahana. This work was supported by grants from the National Institutes of Health (DK082906 to D.F., GM65592 to D.F., GM66492 to R.W.K. and NS047533 to S.M.W.); the Harvard Technology Development Accelerator Fund (D.F.); Merck & Co. (D.F. and R.W.K.); and Johnson & Johnson (D.F. and R.W.K.).

**Author Contributions** B.-H.L. carried out screening and most *in vitro* studies, and M.J.L. chemical analysis and most cell-based assays. R.W.K. and D.F. were responsible for overall design and oversight of the project. S.P., S.E. and N.D. provided skilled assistance in proteasome biochemistry and assays. D.-C.O., C.G. and S.P.G. designed and carried out chemistry studies. P.-C.C., S.M.W. and J.H. provided key reagents and intellectual input. Many authors contributed to preparation of the manuscript.

**Author Information** Reprints and permissions information is available at www.nature.com/reprints. The authors declare competing financial interests: details accompany the full-text HTML version of the paper at www.nature.com/nature. Readers are welcome to comment on the online version of this article at www.nature.com/nature. Correspondence and requests for materials should be addressed to R.W.K. (randy_king@hms.harvard.edu) or D.F. (daniel_finley@hms.harvard.edu).

## METHODS

**Constructs, antibodies and biochemical reagents.** For expression in mammalian cells we used full-length USP14 (WT USP14) and its splice variant lacking exon 4 (USP14(SF)) subcloned into pcDNA3.1 (Invitrogen) as previously described[18]. The USP14(C114A) and USP14(ΔUBL) constructs were generated in the same vector by PCR-mediated mutagenesis. For bacterial expression, glutathione *S*-transferase (GST)–USP14 fusion protein constructs were generated using pGEX-2T (GE Healthcare). For the Flag-tagged version, the cDNAs were subcloned into pDONR223 and subsequently recombined into pCMV4-based destination vectors (ref. 51). Vectors expressing tau (from V. M. Lee), TDP-43 (from F. E. Baralle), ATXN3 (from H. Paulson), Ub-X–GFPs (from M. G. Masucci), cODC–EGFP (from P. Coffino) and luciferase (from M. Kwak) were provided. The pDONR223 vector was provided by M. Sowa and W. Harper. Anti-USP14 and anti-UCH37 antibodies were provided by R. Baker and G. DeMartino, respectively. Sources of other commercial antibodies are as follows: anti-tau (clone TAU-5; Invitrogen); anti-V5 (Invitrogen); anti-cyclin B (Ab-2, Neomarkers); anti-Flag M2 and anti-actin (A5060, Sigma); anti-Ub (UG9510; Enzo Life Sciences), anti-α6 (PW8100; Enzo), anti-α7 (PW8110; Enzo), and anti-RPN13 (PW9910; Enzo); anti-GFP (Ab290, Abcam); anti-T7-HRP (Novagen); anti-HA (12CA5, Roche); IRDye infrared secondary antibodies (Li-Cor). Sources of major biochemical reagents were as follows: IU1 and IU1C (T0502-8593 and T5369385, Enamine); PS-341 (LC Laboratories); epoxomicin and Ub–VS (Boston Biochem); ADP (Calbiochem); MG132, ubiquitin and bafilomycin $A_1$ (Sigma); Suc-LLVY-AMC (Bachem).

**Purification of recombinant USP14.** GST–USP14 (WT and C114A variants) was expressed in *Escherichia coli* strain Rosetta 2 (DE3) cells (Novagen). Cultures were grown at 37 °C until $OD_{600\,nm}$ reached 0.6 to 0.8, and expression was then induced overnight with 1 mM IPTG at room temperature. Cells were harvested in PBS containing protease inhibitors and lysed by French press. The cleared lysates were incubated with GST Sepharose 4B resin (GE Healthcare) at 4 °C for 1 h, and subsequently washed with excess PBS, followed by PBS containing 100 mM NaCl. The GST moiety was removed by thrombin in cleavage buffer (50 mM Tris-HCl (pH 8.0), 150 mM NaCl, 2.5 mM $CaCl_2$ and 0.1% 2-mercaptoethanol) for 3 h at room temperature. GST-tagged USP14 proteins for proteasome binding assays were eluted before thrombin cleavage using elution buffer (10 mM reduced glutathione and 50 mM Tris-HCl (pH 8.0)).

**Native gel electrophoretic mobility assays.** Native gel analysis using purified proteasomes was performed as in ref. 52, with slight modifications. Briefly, 5 pmol of GST, GST–USP14 WT, GST–USP14(C114A), untagged wild-type USP14, or untagged USP14(C114A) was mixed with 1 pmol of human proteasomes for 20 min at 30 °C. Complexes were resolved by 3.5% non-denaturing PAGE for 850 Volt-hours. Proteasomes were visualized using the fluorogenic substrate Suc-LLVY-AMC (Bachem) as described[52]. Both wild-type USP14 and catalytically inactive USP14(C114A) bind to 26S human proteasomes (Supplementary Fig. 2b).

For whole-cell lysate analysis, buffer B (50 mM $NaH_2PO_4$ (pH 7.5), 10% glycerol, 5 mM $MgCl_2$, 0.25% NP-40, 1 mM DTT, 5 mM ATP and 1× protease inhibitor cocktail) was used for lysis, which was carried out on ice for 15 min with intermittent vortexing. Lysates were cleared by centrifugation at 16,000*g* for 10 min at 4 °C. 75 μg of total protein was loaded on a 3.5% polyacrylamide non-denaturing gel, with electrophoresis for 400 Volt-hours at 4 °C. After the in-gel Suc-LLVY-AMC hydrolysis assay (LAS 3000 imaging system, Fujiflim), gels were pre-soaked in transfer buffer containing 0.1% SDS and no methanol for 15 min (refs 53, 54), followed by protein transfer to PVDF and subsequent immunoblotting against CP subunit α6, which were performed as previously described[55].

**Affinity purification of the 26S human proteasome.** Human proteasomes were affinity-purified on a large scale from a stable HEK293T cell line harbouring HTBH-tagged hRPN11 (a gift from L. Huang). The cells were Dounce-homogenized in lysis buffer (50 mM $NaH_2PO_4$ (pH 7.5), 100 mM NaCl, 10% glycerol, 5 mM $MgCl_2$, 0.5% NP-40, 5 mM ATP and 1 mM DTT) containing protease inhibitors. Lysates were cleared, then incubated with NeutrAvidin agarose resin (Thermo Scientific) overnight at 4 °C. The beads were then washed with excess lysis buffer followed by the wash buffer (50 mM Tris-HCl (pH 7.5), 1 mM $MgCl_2$ and 1 mM ATP). For VS-proteasomes, Ub–VS was added to the resin at 1 to 1.5 μM, followed by incubation at 30 °C for 2 h. Residual Ub–VS was removed by washing the beads with at least 20 bed volumes of wash buffer. 26S proteasomes were eluted from the beads by cleavage, using TEV protease (Invitrogen). VS-proteasomes were tested to confirm the elimination of DUB activity using the Ub–AMC hydrolysis assay. Endogenous wild-type USP14 was not found on the proteasome under these purification conditions (see Supplementary Fig. 1).

To purify human proteasomes (together with RP) in the presence of ADP, 'ATP-free' ADP was prepared and used for all the procedures as previously described[53].

**High-throughput screening for USP14 inhibitors.** Screening was conducted at the ICCB-Longwood screening facility (Harvard Medical School). Ten microlitres of recombinant USP14 protein were dispensed into each well of a 384-well low volume plate (Corning) in duplicate, using a Wellmate plate dispenser. 33.3 nl of compound from the library were pin-transferred into the wells using a Seiko pin transfer robotic system, followed by pre-incubation for about 30 min. The last two columns of each plate were used for positive and negative controls for the assay. To initiate the enzyme reaction, 10 μl of VS-proteasome plus Ub–AMC mixture were added to each well, using a Wellmate dispenser. Samples were then incubated for another 45 min. Ub–AMC hydrolysis was measured at Ex355/Em460 using an Envision plate reader (PerkinElmer). The final concentrations of USP14, VS-proteasome and Ub–AMC were 15 nM, 1 nM and 0.8 μM, respectively. The final concentration of test compound was approximately 17 μM. Enzymes and substrates were prepared in Ub–AMC assay buffer (50 mM Tris-HCl (pH 7.5), 1 mM EDTA, 1 mM ATP, 5 mM $MgCl_2$, 1 mM DTT, and 1 mg $ml^{-1}$ ovalbumin). The sources of compound libraries used for screening were as follows: Maybridge, Asinex, ActiMol TimTec, ChemBridge, ChemDiv, Enamine and MMV1 (natural product extracts).

Primary hits were defined by 'robust' *Z*-score analysis as previously described (Supplementary Fig. 7 and ref. 56). In summary, the raw measurements of each sample from two replicates were averaged, and then *Z*-score was calculated by $(X_i - X)/\mathrm{MADe}$, where $X_i$ is the averaged raw measurement of each sample, $X$ is the median, and MADe is an adjusted median absolute deviation for each replicate plate. This normalization was performed for each plate to adjust for possible plate-to-plate variation. Strong hits were defined as *Z*-score $< -10$, medium hits as $-10 < Z < -7$, and weak hits as $-7 < Z < -3.5$.

**Secondary screening.** A total of 312 primary hits were first tested, in a 384-well plate format, for quenching the fluorescence of AMC amine to eliminate false positives. To exclude quenching compounds that only affect AMC fluorescence, each compound (17 μM) was first tested for quenching of AMC amine (50 nM). Quenchers were retested for inhibition of proteasome-associated USP14 activity and the strength of this effect was compared to their quenching effect in a dose- and time-dependent manner. Pure quenchers were thus scored as false positives and excluded from further analysis.

To test the specificity of potential USP14 inhibitors, each candidate was first counter-screened against human IsoT, a DUB that is closely related to USP14. Only compounds having significant activity for USP14 over IsoT were considered for further analysis with a panel of other human DUBs. IsoT and BAP1 were provided by K. Wilkinson, and UCH37 by K. Walters. UCH-L1, UCH-L3, USP2 catalytic domain (CD), USP7(CD) and USP15 were purchased from Boston Biochem. The final concentrations of DUBs in these reactions were as follows: USP14 (30 nM in the presence of 2.5 nM VS-proteasome), IsoT (1.5 nM), UCH37 (0.7 nM), BAP1 (2.5 nM), UCH-L1 (8 nM), UCH-L3 (0.3 nM), USP2 (50 nM), USP7 (50 nM) and USP15 (50 nM). To activate IsoT, 0.02 μM ubiquitin was added to the reaction. UCH37 was assayed in purified recombinant form in Fig. 2b, c. The proteasome-associated form of UCH37 was also assayed against IU1, with equivalent results (Supplementary Fig. 8b). In these experiments, we used proteasomes affinity-purified from tagged HEK293 cells without Ub–VS treatment, at both 0.5 and 1.0 nM. Ub–AMC (0.1 to 1 μM) was used as substrate for all quantitative DUB assays.

**$IC_{50}$ value determination.** To measure $IC_{50}$ values, various concentrations of IU1 (100 μM to 50 nM for proteasome-bound USP14, and 2 mM to 50 nM for IsoT and UCH37) were pre-incubated with corresponding DUBs for 30 min. The reaction was initiated by adding 1 μM of Ub–AMC. These experiments were done in triplicate and represented as mean ± s.d. Fluorescence was measured by monitoring the reactions at room temperature for 45 min in real time using an Envision plate reader. $IC_{50}$ determination for IU1C was performed with 2 mM to 50 nM of compound. To obtain a dose–response curve, the per cent inhibition for each reaction was first determined, and then curve fitting was performed by the four parameter logistic model or the three parameter fixed bottom model using SigmaPlot 9.0 according to guidelines from NIH Chemical Genomics Center (http://ncgc.nih.gov/guidance/manual_toc.html).

**Ubiquitination and purification of $Sic1^{PY}$.** Ubiquitination of $Sic1^{PY}$ was carried out essentially as described[32], but with some modifications. The conjugation mixture contained 1.2 μM $Sic1^{PY}$, 0.17 μM Uba1, 0.62 μM Ubc4, 0.71 μM Rsp5 and 20 μM ubiquitin, in a buffer of 50 mM Tris-HCl (pH 7.4), 100 mM NaCl, 1 mM DTT, 5 mM ATP and 10 mM $MgCl_2$. Conjugation proceeded for 100 min at 25 °C. To purify the conjugates, they were absorbed to Qiagen Ni-NTA resin, washed with buffer (50 mM Tris-HCl (pH 8.0), 50 mM NaCl and 40% glycerol), eluted with 200 mM imidazole in wash buffer, and dialysed into wash buffer containing 10% glycerol.

***In vitro* protein degradation and chain-trimming assays.** Purified human proteasomes (4 to 5 nM) were incubated with polyubiquitinated cyclin B ($Ub_n$–CCNB; ~40 nM final) or polyubiquitinated $Sic1^{PY}$ ($Ub_n$–$Sic1^{PY}$; ~240 nM final)

in proteasome assay buffer (50 mM Tris-HCl (pH 7.5), 5 mM $MgCl_2$ and 5 mM ATP). Where indicated, purified recombinant USP14 was incubated with proteasome for 5 min before initiating the reaction. To test the effect of IU1, 34 or 75 μM IU1 was pre-incubated with USP14 for 5 min before adding proteasome. Proteasome inhibitor cocktail (5 μM each of PS-341 and epoxomicin) was added 10 min in advance of the assay to inhibit the catalytic activity of proteasomes. For chain-trimming assays with ADP, the reaction was performed in the presence of ADP, with the proteasome-containing sample purified in the presence of ADP. This sample was pre-incubated with IU1 for 30 min (rather than 5 min) for Supplementary Fig. 14e. Reactions were terminated by adding 5× SDS–PAGE sample buffer and subsequently subjected to SDS–PAGE/immunoblot analysis using anti-cyclin B1 polyclonal antibody or anti-T7 HRP antibody. $Ub_n$–CCNB was prepared as previously described[33].

**IU1 reversibility test.** The reversibility of IU1 inhibition of USP14 was examined by gel filtration using Centrispin-10 spin columns (Princeton Separations). 60 nM of USP14 and 5 nM of VS-proteasome were treated with vehicle or 100 μM IU1 for each indicated time point, at room temperature. The protein complex was then centrifuged through a gel-filtration column and assayed for DUB activity by adding Ub–AMC (1 μM). Each error bar for Fig. 2b–d indicates standard deviation of three comparable experiments. To test IU1 inhibition of proteasome-bound USP14 for a prolonged incubation, the decay of activity or the stability of the enzyme complex was also investigated up to 8 h (Supplementary Fig. 13c). The DUB activity of each vehicle-treated control was normalized to 100%, and IU1-treated enzyme activity was expressed as a percentage of inhibition for each control. For Supplementary Fig. 13d, DUB activity was further normalized to Suc-LLVY-AMC hydrolytic peptidase activity. To confirm the reversibility of IU1, USP14 (60 nM) and VS-proteasome (5 nM) were incubated with vehicle or 100 μM of IU1 for 2 h at 4 °C. Each sample was then subjected to three rounds of ultrafiltration, using a Microcon-YM3 filter (3-kDa cutoff, Millipore). After each spin, the protein complex was re-suspended to the original volume and assayed for DUB activity. In some cases, the filtrate before and after centrifugation was saved for SDS–PAGE and immunoblot analyses using anti-USP14 and anti-α7 antibodies (see Supplementary Fig. 13e).

**Mammalian cell cultures and transient expression.** Homozygous *Usp14* null mice have been previously generated by a gene-trap strategy, which exhibited embryonic lethality at approximately E13.5 (ref. 19). The gene trap allele, $Usp14^{rrk114}$, is referred to here as $Usp14^{-/-}$. Cultures of primary mouse embryonic fibroblasts (MEFs) were established from E12.5 $Usp14^{-/-}$ and littermate wild-type embryos produced through intercrosses of 129/BL6 $Usp14^{+/-}$ mice. Primary MEFs were immortalized using the pEF321-T plasmid, which expresses Simian Virus 40 (SV40) large T-antigen[57,58]. MEFs, human kidney cells (HEK293) and HeLa cells were grown in DMEM supplemented with 10% FBS, 2 mM glutamine and 100 units $ml^{-1}$ penicillin/streptomycin. Cells were transfected with 2–4 μg of total plasmid DNA in a 6-well culture plate for 4 h using LipofectAMINE 2000 (Invitrogen) when cells were >95% confluent or at a density of $10^6$ cells per well. Cell lysates were prepared 36–48 h after transfection in RIPA buffer and used for immunoblotting. In a given panel, each lane is loaded with extract from an equal cell number, generally corresponding to 10–20 μg per lane, or 1/10 of the sample recovered from one well of a 6-well plate. For chase analysis, MEFs were treated with 75 μg $ml^{-1}$ cycloheximide and samples were isolated at chase times 0, 0.5, 1, 2 and 4 h. Autophagic vacuole formation was inhibited by the treatment of 200 μM of bafilomycin $A_1$ for 6 h, which was verified by marked increase of transiently expressed mCherry-NBR1 (ref. 59). For quantitative immunoblot, proteins were visualized by infrared fluorescence antibodies using an Odyssey Imaging System (Li-Cor) and quantified using Odyssey software version 3.0 from three independent experiments. Tau signal was normalized to that of endogenous actin and values are represented as mean ± s.d.

**Quantitative RT–PCR analysis.** Total RNA from cultured cells was prepared using the TRIzol reagent (Invitrogen), followed by further purification through RNeasy mini-column (Qiagen) with on-column DNase I treatment. 250 ng of extracted RNA was used for quantitative RT–PCR in a LightCycler Carousel-Based System (Roche), using RNA Master SYBR Green I (Roche) as reporter dye. Reverse transcription was performed at 61 °C for 20 min and amplifications were performed for 40 cycles of 95 °C for 5 s, 60 °C for 20 s, and 72 °C for 30 s. Each mRNA level was normalized to that of GAPDH and the values were plotted as means ± s.d. of three independent experiments. Primer sequences used were as follows: for tau, forward 5′-AAGGTGACCTCCAAGTGTGG-3′ and reverse 5′-GGGACGTGGGTGATATTGTC-3′; for TDP-43, forward 5′-ATGGAAAA CAACCGAACAGG-3′ and reverse 5′-CAGTCACACCATCGTCCATC-3′; for GFAP, forward 5′-AGGAAGATTGAGTCGCTGGA-3′ and reverse 5′-ATACT GCGTGCGGATCTCTT-3′; for USP14, forward 5′-AAATGGCTTCAGCGC AGTAT-3′ and reverse 5′-TTCACCTTTCTCGGCAAACT-3′; for UbB, forward 5′-AGACCATCACCCTGGAAGTG-3′ and reverse 5′-AGGGTCGACTCCTT CTGGAT-3′; for α5, forward 5′-CGTGTGGCCTTTGGGAAC-3′ and reverse 5′-CACAACCTATATGAGCATCG-3′; for α7, forward 5′-ACAGTGGAGGA CCCAGTGAC-3′ and reverse 5′-CAATTAGGGCCGAGATACCA-3′; for GAPDH, forward 5′-GAGTCAACGGATTTGGTCGT-3′ and reverse 5′-GAC AAGCTTCCCGTTCTCAG-3′.

**Determination of cell viability.** Cell viability was assessed by the MTT assay[60]. Briefly, cells were grown in 96-well plates at a density of $2 \times 10^4$ cells per well. After IU1 or DMSO treatment, thiazolyl blue tetrazolium bromide (MTT, Sigma Aldrich) was added to each well of cells (final 0.5 mg $ml^{-1}$) and incubated for 1.5 h at 37 °C in a humidified atmosphere of 95% air/5% $CO_2$. DMSO was added to solubilize the blue MTT-formazan product and the sample was incubated for a further 30 min at room temperature. Absorbance of the solution was read at a test wavelength of 570 nm against a reference wavelength of 630 nm. $IC_{50}$ values were determined using GraphPad Prism version 4.0 (GraphPad Software, Inc.). For cell survival upon oxidative stress, cells were pre-treated with 50 μM of IU1 for 2 h and a series of concentrations of menadione was then added, followed by incubation for 4 h before the MTT assay. Data in MTT assays represent mean values ± s.d. from three independent experiments. Apoptotic cells induced by IU1 were detected by TUNEL assay[61] using a fluorescence-based *in situ* cell death detection kit (Roche) and DAPI (Invitrogen) counterstaining according to the manufacturers' protocols. The extent of fluorescein-labelled DNA-strand breakage was evaluated from at least 1,000 cells out of ten different ×200 fields. For live-cell proliferation measurement, HeLa cells and MEFs were plated on 24-well plates (BD Biosciences) at around 35,000 cells per well or no more than 30% confluency. The next day, various concentrations of IU1 or the equivalent amounts of vehicle were added to each well in duplicate. Plates were then placed into an IncuCyte instrument (Essen Instruments) to automatically image cells every 2 h and measure confluence. Cells were imaged for 72 h or until they reached full confluence.

**Oxidized protein analysis.** Oxidized proteins were detected using the OxyBlot protein oxidation detection kit (Millipore). Total proteins from cells were isolated after treatment with 300 μM of menadione for 1 h, 75 μM of IU1 for 4 h, and/or proteasome inhibitors (20 μM of MG132; 10 μM of PS-341) for 4 h, and 15 μg of protein was used for derivatization with 2-4-dinitrophenyl hydrazine (DNPH) for 25 min. Samples were resolved by SDS–PAGE and anti-DNP antibody was used for subsequent immunoblotting. IU1 does not inactivate menadione, as determined by LC-MS (data not shown).

**Compound analysis.** $^1$H spectra were acquired on a Varian Inova 600 MHz spectrometer. Chemical shifts are reported as parts per million (p.p.m.) downfield from tetramethylsilane. Data are reported as follows: chemical shift, multiplicity (s = singlet, d = doublet, t = triplet, m = multiplet, br = broad), coupling constant and integration. Analytical LC-MS chromatography was performed using the Agilent 1200 Series HPLC/6130 Series mass spectrometer with a gradient solvent system from 10% to 50% $CH_3CN$ (0.1% formic acid) over 15 min (IU1) or 10% to 100% $CH_3CN$ (0.1% formic acid) over 23 min (IU1C). The collected LC-MS profiles were further analysed by extracting specific ions such as 301.0 (IU1) and 315.0 (IU1C) in the positive ion MS mode. IU1 and IU1C were determined to be >99% pure by LC-MS. High-resolution mass spectrometry (HRMS) was performed by the University of Illinois Mass Spectrometry Laboratory.

$^1$H-NMR (600 MHz, DMSO-$d_6$) of IU1: $\delta = 7.38$ (m, 4H), 6.44 (s, 1H), 3.65 (s, 2H), 2.57 (m, 4H), 2.21 (s, 3H), 1.93 (s, 3H), 1.70 (m, 4H) p.p.m. HRMS (ESI) = $m/z$ calculated for $C_{18}H_{21}FN_2O$ $[M+H]^+$ 301.1716, found 301.1729.

$^1$H-NMR (600 MHz, DMSO-$d_6$) of IU1C: $\delta = 7.38$ (m, 4H), 5.93 (s, 1H), 4.21 (br, 2H), 2.82 (br, 2H), 1.97 (s, 3H), 1.96 (s, 3H), 1.62 (m, 4H), 1.02 (m, 1H), 0.92 (d, $J = 6.0$ Hz, 3H) p.p.m. HRMS (ESI) = $m/z$ calculated for $C_{19}H_{23}FN_2O$ $[M+H]^+$ 315.1873, found 315.1872.

For the extraction of internalized small molecules, cells were washed 3× with PBS and lysed in LC-MS lysis buffer A (10 mM $K_2HPO_4$ (pH 7.5), 0.1 mM EDTA, 0.5 mM EGTA, 0.5% Triton X-100, and 1 mM DTT) containing 1× Complete protease inhibitors and 1× PhosSTOP phosphatase inhibitors (Roche), followed with the addition of 2.5 vol. ethyl acetate. The organic phase was separated from the aqueous phase and dried with anhydrous sodium sulphate. The extracts were dried *in vacuo*, then re-suspended in 200 μl of methanol for LC-MS analysis. LC-MS data were obtained using an Agilent series 1200 LC/6130 MS system with a reversed-phase $C_{18}$ column (Phenomenex Luna $C_{18}$[2], 4.6 mm × 100 mm, 5 μm) and a $CH_3CN/H_2O$ gradient solvent system, beginning with 10% aqueous $CH_3CN$ and ending at 50% $CH_3CN$ at 15 min. 10 μl of each sample was injected for each analysis. The collected LC-MS profiles were further analysed by extracting specific ions such as 301.0 (IU1) and 172.2 (menadione) in the positive ion MS mode. IU1 and menadione were eluted at 8.8 min and 14.9 min, respectively. To determine the excluded cell volume, [$^3$H]methoxyinuline (25 μCi) was added to cell pellets before collection to measure extracellular volume[62]. The intracellular concentrations of IU1 were normalized by cell number.

**Reporter gene assays.** To examine the promoter activities of *Psmb5* in the presence or absence of IU1, wild-type and $Usp14^{-/-}$ MEFs seeded on 6-well

plates were transfected with 3 μg of pGL3-Psmb5-luciferase plasmid, which contains a 1-kb segment from the promoter of the murine *Psmb5* gene[63,64]. After 24 h, cells were incubated with 25 μM or 50 μM of IU1 for 6 h, and then luciferase activities were measured using a luciferase reporter assay system (Promega). The luminometer was a Wallac 1420 Workstation. Values were normalized to that of a pGL3-luciferase control transfection, with protein concentration determined by the Bradford assay, and presented as means ± s.d. ($n = 3$).


51. Sowa, M. E., Bennett, E. J., Gygi, S. P. & Harper, J. W. Defining the human deubiquitinating enzyme interaction landscape. *Cell* **138,** 389–403 (2009).
52. Elsasser, S., Schmidt, M. & Finley, D. Characterization of the proteasome using native gel electrophoresis. *Methods Enzymol.* **398,** 353–363 (2005).
53. Kleijnen, M. F. *et al.* Stability of the proteasome can be regulated allosterically through engagement of its proteolytic active sites. *Nature Struct. Mol. Biol.* **14,** 1180–1188 (2007).
54. Kusmierczyk, A. R., Kunjappu, M. J., Funakoshi, M. & Hochstrasser, M. A multimeric assembly factor controls the formation of alternative 20S proteasomes. *Nature Struct. Mol. Biol.* **15,** 237–244 (2008).
55. Park, S. *et al.* Hexameric assembly of the proteasomal ATPases is templated through their C termini. *Nature* **459,** 866–870 (2009).
56. Malo, N., Hanley, J., Cerquozzi, S., Pelletier, J. & Nadon, R. Statistical practice in high-throughput screening data analysis. *Nature Biotechnol.* **24,** 167–175 (2006).
57. Kobayashi, H. *et al.* Hrs, a mammalian master molecule in vesicular transport and protein sorting, suppresses the degradation of ESCRT proteins signal transducing adaptor molecule 1 and 2. *J. Biol. Chem.* **280,** 10468–10477 (2005).
58. Kuma, A. *et al.* The role of autophagy during the early neonatal starvation period. *Nature* **432,** 1032–1036 (2004).
59. Mizushima, N., Yoshimori, T. & Levine, B. Methods in mammalian autophagy research. *Cell* **140,** 313–326 (2010).
60. Mosmann, T. Rapid colorimetric assay for cellular growth and survival: application to proliferation and cytotoxicity assays. *J. Immunol. Methods* **65,** 55–63 (1983).
61. Li, X., Traganos, F., Melamed, M. R. & Darzynkiewicz, Z. Single-step procedure for labeling DNA strand breaks with fluorescein- or BODIPY-conjugated deoxynucleotides: detection of apoptosis and bromodeoxyuridine incorporation. *Cytometry* **20,** 172–180 (1995).
62. Jordan, M. A., Thrower, D. & Wilson, L. Mechanism of inhibition of cell proliferation by Vinca Alkaloids. *Cancer Res.* **51,** 2212–2222 (1991).
63. Chondrogianni, N. *et al.* Central role of the proteasome in senescence and survival of human fibroblasts. *J. Biol. Chem.* **278,** 28026–28037 (2003).
64. Kwak, M. K. *et al.* Antioxidants enhance mammalian proteasome expression through the Keap1-Nrf2 signaling pathway. *Mol. Cell. Biol.* **23,** 8786–8794 (2003).